Published as:
Potgieter, G., Focke, W. W., Del Fabbro, O., Labuschagné, G. D. & Kelly, C. 2016b. Fluoroelastomer pyrotechnic time delay compositions. Journal of Thermal Analysis and Calorimetry, 126, 1363-1370.

Fluoroelastomer pyrotechnic time delay compositions

Gerard Potgieter[a], Walter W Focke[a], Olinto Del Fabbro[a], George D Labuschagné[b] and Cheryl Kelly[b]

[a]Institute of Applied Materials, Department of Chemical Engineering, University of Pretoria, Private Bag X20, Hatfield 0028, Pretoria, South Africa
[b]Research and Technology, AEL Mining Services, PO Modderfontein, 1645, South Africa

Abstract

The feasibility of aluminium or magnalium filled fluoropolymer Viton B as an open-burn time delay was investigated. Film samples with a thickness of 245 ± 21 μm. were prepared via a slurry casting process. Fuel filler content was varied from 20 to 60 wt.%. The films retained the elastic properties of the parent polymer except that the elongation at break decreased rapidly with increasing filler content. Sensitivity tests showed that the films were insensitive to ignition by friction and impact. EKVI thermodynamic simulations showed that, for both systems, the maximum energy output is ca. 8.3 MJ kg^{-1}. Energy measurements indicated that the maximum energy output occurred in the range 30 to 40 wt.%. Maximum burn rates of 82 mm s^{-1} and 40 mm s^{-1} were achieved using a magnalium and flake aluminium as fuels respectively.

Keywords: Pyrotechnic; time delay; fluoropolymer; burning rate

1. Introduction

Chemical time delay elements are used to ensure controlled detonation of charges in blasting operations [1]. They consist of pyrotechnic compositions filled in small-diameter tubes of varying length [2]. Conventional pyrotechnics are based on intimate mixtures of two or more powders capable of exothermic redox reactions [3]. The oxidizing agent is usually a metal oxide and the fuel a metal or metalloid. A constant burning rate is desired to ensure that the transmission of an initiation impulse occurs in a precisely adjustable time interval. Thus delay compositions that burn at a constant predetermined rate in an essentially gasless fashion are preferred [4]. The actual combustion event in the column is governed by a number of parameters [5]. The thermal diffusivity of the mixture is always important as combustion wave propagation depends on continuous re-ignition of adjacent layers along the burning path. The actual time delay realized is determined by the nature of the reactants, the stoichiometry of the pyrotechnic composition, the dimensions of the column, i.e. its length and diameter, and the material of construction of the tube [1, 5].

Theoretical models for the self-propagating layer-to-layer reactions in the solid phase have been developed [6-13]. They link the rate of progression of the reaction zone through the mixture of the reactants in the form of a cylinder, with the chemical composition and some of the physical properties of the powders, the state of subdivision of the powders, and the reaction kinetics between the constituents [6].

Good mixing and adequate particle-particle contact between reactants (i.e. efficient particle packing) is a prerequisite for stable and reproducible burning. This, however, involves challenges as it is difficult to ensure that unlike particle contacts predominate. An intriguing possibility is to replace at least one of the particulate reactants with a suitable polymer. One option is to use a perfluorinated polymer as oxidant in combination with a metallic fuel. This could make it possible to manufacture times delays using polymer converting processes such as extrusion. Indeed, poly(tetrafluoroethylene) (PTFE) is used in pyrotechnics but unfortunately it is also a refractory material (Nielson, Truitt, & Rasmussen, 2005). It is therefore used in powder form and powder processing techniques must be

applied. Filled PTFE can only be continuously processed into billets using ram extrusion (Ebnesajjad, 2000). This technique, requires a sintering step that raises concerns over the safety of processing such pyrotechnic compositions. However, fluoropolymers exist that can be solution- and/or melt-processed. Examples include copolymers of tetrafluoroethylene (TFE), hexafluoropropylene (HFP) and 1,1-difluoroethylene (VDF).

The aim of this preliminary study was to explore the possibility of using fluoropolymer-based compositions as pyrotechnic time delay elements in a safe and reproducible manner. Furthermore, the major parameters that affect the performance of such compositions had to be identified. The controlled variables were the nature of the reducing agent, the fuel filler morphology and the filler loading (stoichiometry). The performance was analysed by measuring the energy output, burn rate, pressure profile generated, mechanical properties and the products formed during reaction.

2. Experimental

2.1. Modelling

Thermodynamic simulations were done using the EKVI thermodynamics software package. The effect of reagent stoichiometry on the product spectrum and energy output, i.e. adiabatic reaction temperature, were simulated at 30 bar. The fuels considered were magnalium and aluminium.

2.2. Materials

Viton® B-50 fluoropolymer pellets containing 68% fluorine were donated by Necsa. This is a copolymer of vinylidene fluoride, hexafluoropropylene and tetrafluoroethylene and hence it was categorized as FKM Type 2 according to ISO 1629:2013. FTIR spectroscopy confirmed the sample identity.

Aluminium flake, grade APS 11 micron, was purchased from AlfaAesar. This grade had a purity of 99.7% on a metals basis. Magnalium powder was manufactured by the CSIR. It contained 53 % magnesium and 47% aluminium. Atomised aluminium powder (grade A120FB) was supplied by Ginman. The latter two powders were each passed through a 325 mesh sieve and the lower fractions were retained.

2.3. Sample preparation

Pyrotechnic films were made using a solution casting process. The Viton B was dissolved in ethyl acetate at room temperature at a solids content of 16.6 wt.%. Predetermined amounts reducing agent powders were added and suspended in this solution. Homogeneity of the composition was ensured by mixing at the maximum stirring speed with a magnetic stirrer. Films were cast in shallow Teflon-coated trays and allowed to dry for 24 h at room temperature. Final film thickness was 245 ± 21 μm. The fuel content of the dry material was varied from 20 to 60 wt.% in 10 wt.% increments.

2.4. Material characterisation

Particle size was determined with a Malvern Mastersizer Hydro 2000MY instrument. XRD analysis was performed on a PANalytical X-pert Pro powder diffractometer. The instrument featured variable divergence and receiving slits and an X'celerator detector using Fe filtered CoKα radiation (0.178901 nm). XRD data analysis was done using X'Pert Highscore plus software. The ARL Perform'X Sequential XRF with Uniquant software was used for XRF analyses. The samples were prepared as pressed powder briquettes. Scanning electron microscopy (SEM) images were recorded on a Jeol JSM-5800 microscope.

Thermogravimetric analysis was performed on a Perkin Elmer 4000 TGA in air flowing at 50 mL min^{-1}. The sample size was ca. 15 mg. The temperature was scanned from 25 °C to 900 °C at a scan

rate of 10 °C min^{-1}. The sample was held at that temperature for 30 min to burn off the carbon residue. The residues were imaged with the SEM.

A Parr Instruments 6200 bomb calorimeter was used for energy output measurements. Tests were conducted at 30 bar in a helium atmosphere. The compositions were ignited using a nichrome wire. The variation of the differential pressure (ΔP) with time was measured using a NI piezoelectric pressure transducer connected to the Parr pressure recording system. The sampling rate was 2.5 kHz and 30000 data points were recorded per run. The sample size was kept constant at 0.30 g. The combustion residues were recovered and the phase content and chemical composition determined using XRD and XRF respectively.

Sensitivity tests were performed on compositions containing 30 wt.% fuel. The BFH-10 Bam fall hammer impact sensitivity test and the FSKM 50-20K bam friction sensitivity tests were performed.

2.5. Burning rate measurements

The film strips measuring 7.5 mm wide by 50 mm long were cut from the films. Owing to the elastomeric nature of the films, the thickness was determined by sandwiching them between reinforced phenolic sheets of known thickness. Samples were ignited at one end using a 40 W Synrad CO_2 laser as ignition source. The laser power output was set to 12 W. A GoPro camera was used and the open flame burning event was recorded at a rate of 120 frames per second at a resolution of 1280 × 720 pixels (720p). Video data was analysed using Microsoft movie maker at 0.125× playback speed in order to determine the burning rate.

2.6. Mechanical properties

A Lloyds Instruments LRX machine fitted with a 50 N load cell was used for tensile testing. The gauge length was set to 100 mm and the cross-head speed was 100 mm min^{-1}.

Table 1. Fuel particle sizes

Size, μm	Al flake	Atomised Al	Raw magnalium	Sieved magnalium
d_{10}	3.0	5.4	4.8	5.6
d_{50}	16.0	20.8	18.3	19.6
d_{90}	88.8	68.1	59.9	45.2

3. Results

3.1. Powder characterization

Fig. 1 shows SEM micrographs and **Fig. 2** the particle size distributions of the fuel powders. The d_{10}, d_{50} and d_{90} particle size of the as-received magnalium powder and the aluminium flake, sieved atomised aluminium and sieved magnalium are reported in Table 1. The flake aluminium powder featured a distinct bimodal particles size distribution. X-ray fluorescence indicated that the magnalium contained 57 wt.% aluminium and 43 wt.% magnesium on a metals basis.

3.2. EKVI simulations and calorimetric results

The energy output of compositions based on aluminium are compared to EKVI predictions in **Fig. 3**. The model predicted an approximate linear increase in energy output up to the global maximum at 25 wt.% aluminium, corresponding to an energy output of 8.29 MJ kg^{-1}. Beyond that there was a continuous decrease in energy output. The measured energy outputs of compositions containing aluminium flake or atomised aluminium powders are also shown in **Fig. 3a**. The highest energy output was realised at 30 wt.% aluminium for both compositions. There was an unexpected difference in the measured energy output of the two compositions between 30 wt.% aluminium and 50 wt.% aluminium. This anomaly is attributed to incomplete combustion of the composition containing aluminium flakes. This was confirmed by inspecting the combustion residue. The measured values for both compositions, however, followed a similar trend to the simulated results.

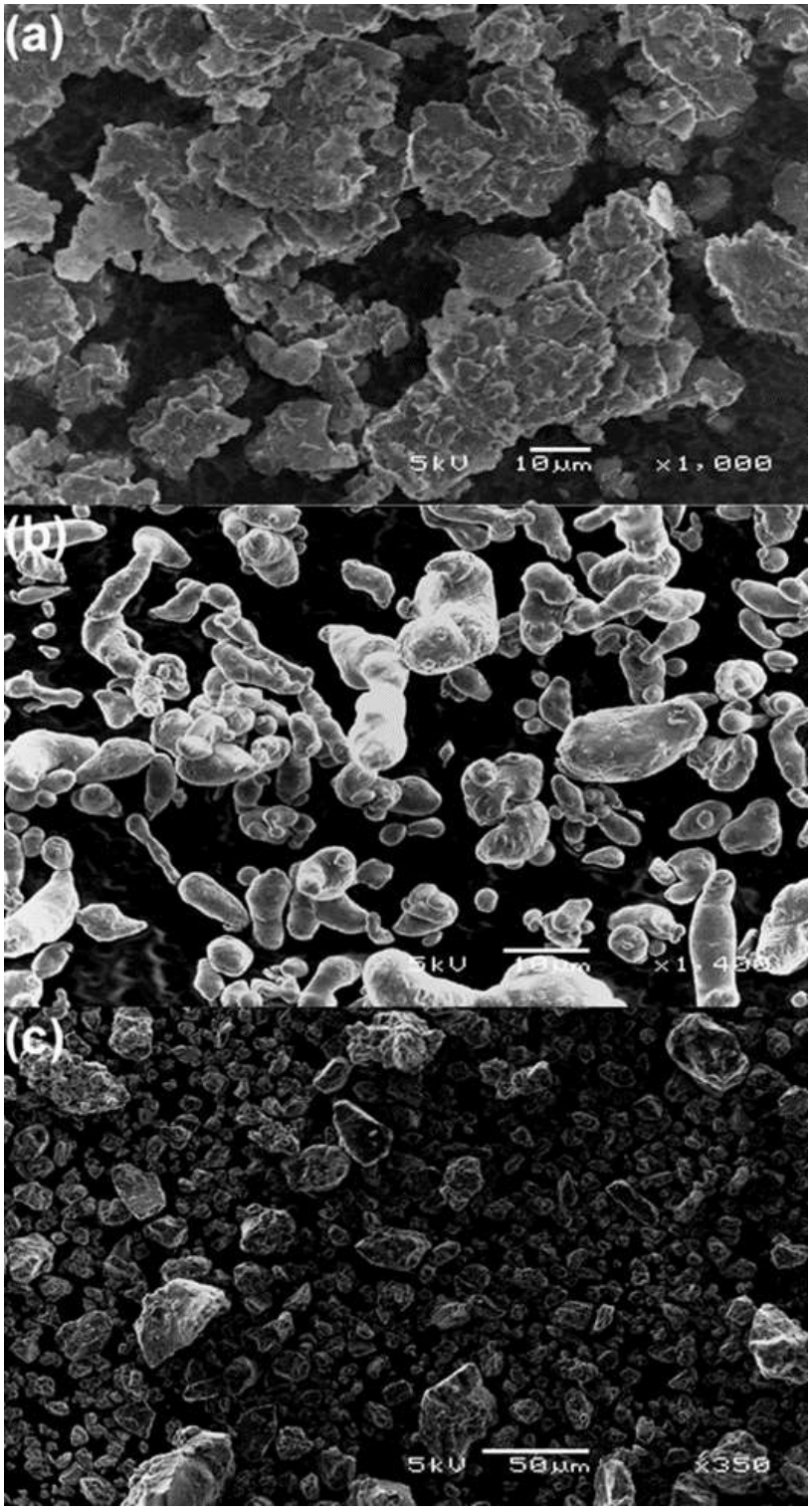

Fig. 1 Scanning electron micrographs of the fuel powders. (a) Aluminium flake; (b) sieved atomised aluminium, and (c) sieved magnalium powder

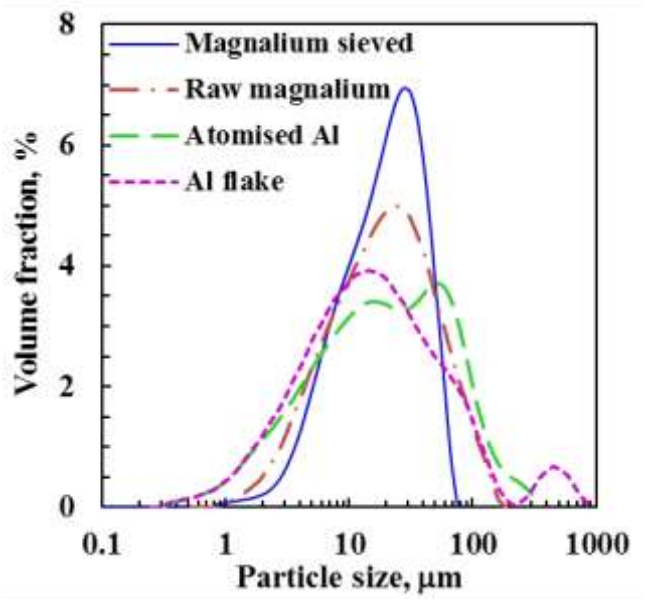

Fig. 2 Particle size distributions of the fuel powders

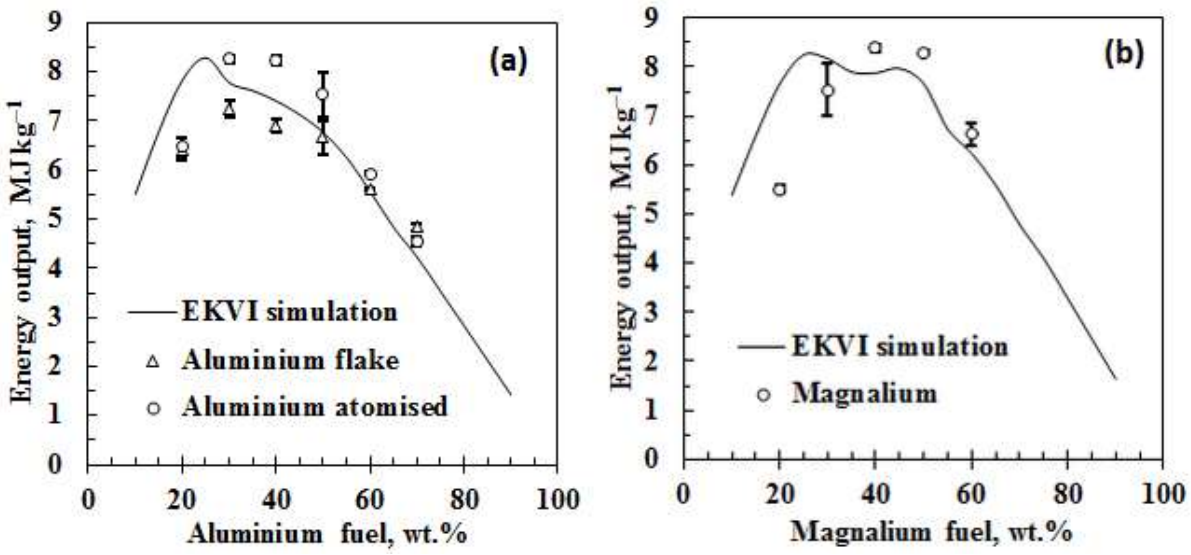

Fig. 3 Energy output comparison of compositions based on aluminium or magnalium as fuel with Viton B as oxidant

The energy output of magnalium/Viton B compositions are compared to EKVI simulation results in **Fig. 3b**. The variation with fuel content, of the experimental values and the simulated results, followed the same trends. However, the experimental results appear shifted to higher fuel content with

the energy output reaching its maximum value of 8.3 MJ kg^{-1} between 40 wt.% and 50 wt.% magnalium.

3.3. Pressure (ΔP) analysis

Fig. 4 records typical differential pressures recorded for the combustion events in the bomb calorimeter. The highest pressure differential was recorded for the 30 wt.% magnalium composition. Beyond this fuel content the ΔP decreased. Similar ΔP results were obtained with the atomised aluminium compositions. However, compositions based on the aluminium flake powder showed a maximum ΔP at about 50 wt.% aluminium content. The absence of residual pressure indicated that the pressure increase was caused, in the main, by the heating of the helium gas used as inert atmosphere rather than gas generated by the reactions.

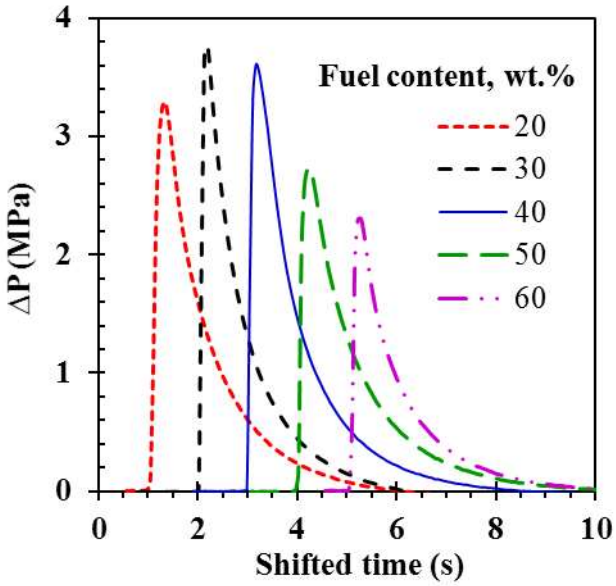

Fig. 4 Pressure (ΔP) profiles for magnalium compositions. Note that the pressure curves were shifted to the right to aid visualization

The pressure-time data was filtered and splined so that the derivative could be determined. The results are summarised in Table 2. The measured energy output was included for comparison. The largest gradient was found for the 30 wt.% magnalium composition, indicating the highest instantaneous rate of temperature change. The flake aluminium composition, however, had the shortest average time to maximum over the range, indicating the highest average reaction rate.

Table 2. Bomb calorimeter pressure data for the Viton B composition

Fuel type	**Fuel**	**ΔP_{max}**	**Time to ΔP_{max}**	**$d(\Delta P)/dt_{max}$**	**Enthalpy**
	wt.%	MPa	s	MPa s^{-1}	MJ kg^{-1}
Magnalium	20	3.30	0.27	22	5.50
	30	3.10	0.24	40	7.52
	40	3.61	0.185	34	8.38
	50	2.73	0.18	25	8.29
	60	2.32	0.185	19	6.62
Aluminium flake	20	-	0.24-0.35	24	6.42
	30	3.07	0.23	26	6.57
	40	3.72	0.21	35	6.67
	50	3.43	0.13	33	6.66
	60	2.91	0.18	29	5.61
Atomised aluminium	20	3.59	0.35	15	6.47
	30	3.48	0.35	30	8.26
	40	3.05	0.23	23	8.23
	50	3.52	0.18	32	7.54
	60	2.92	0.20	32	5.93

3.4. Burning rate

Fig. 5 shows the effect of stoichiometry on the burning rate. Sustained burning at 20 wt.% fuel was only possible using compositions based on the Al flake powder. The burning rate of all compositions increased with increasing fuel content. The 40 wt.% magnalium was the only exception. The fastest burning rate was obtained using the magnalium composition at stoichiometric ratio's between

50 wt.% and 60 wt.%. The slowest sustained burning rate of 12.4 mm s^{-1} was achieved using 30 wt.% atomised aluminium powder.

The effect of particle size on burning rate was tested by filling Viton B with 50 wt.% magnalium. The particles used had d_{50} of 20.4 µm and 11.0 µm. The results shown in **Fig. 5b** reveal that the composition using the 20.4 µm particles had a burn rate that was more than twice that of the 11 µm particles.

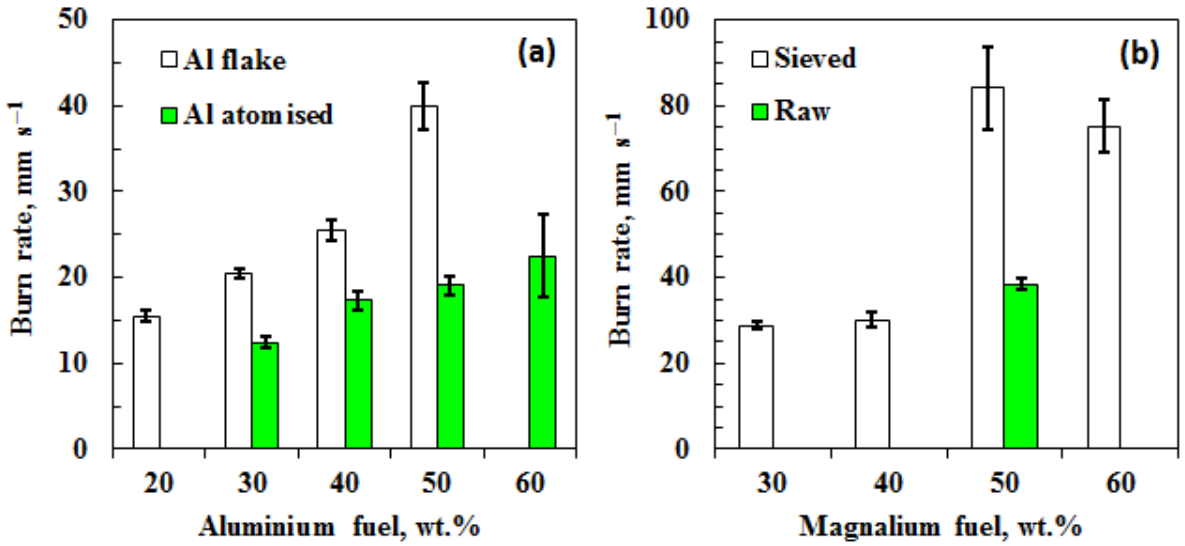

Fig. 5 Burn rate as a function of stoichiometry. (a) Aluminium as fuel, and (b) magnalium as fuel

3.5. X-ray diffraction/fluorescence

Quantitative XRD analysis was performed on the reaction products recovered from the bomb calorimeter tests. Quantitate analysis of the reaction products obtained with magnalium as fuel was not possible as there were unidentified reflections in the corresponding XRD spectra. However, the main reaction products identified were graphite, aluminium fluoride, and magnesium oxide. The major products found with aluminium as fuel were aluminium carbide, aluminium fluoride, graphite and unreacted aluminium. Small amounts of aluminium fluoride hydroxide ($Al_xF(OH)_{3-x}$) were also detected. Its formation was attributed to the presence of adventitious moisture. A large amorphous

fraction was also present, constituting up to a third of the total products. Table 3 summarises the quantitative analyses done on compositions based on flake-like aluminium particles and spherical aluminium particles respectively.

Table 3 also lists the product spectra predicted by the EKVI thermodynamic software for comparison. The XRD results showed lower aluminium carbide and aluminium fluoride formation than predicted for both compositions. This is coupled with lower than predicted aluminium conversion. The large difference between the measured and predicted graphite content is attributed to the formation of amorphous carbon (disordered graphite) due to the presence of hydrogen in the reaction (Ferrari & Robertson, 2000). Perhaps overall the match only appears poor owing to the uncertain composition of the amorphous phases.

Table 3. Quantitative XRD analysis of the reaction products of compositions using flake-like aluminium particles compared with the predictions from the EKVI thermodynamics package

Fuel type:	**Flake**			**Atomised**			**EKVI Predictions**		
Formula	20	40	60	20	40	60	20	40	60
Al_4C_3	1.16	9.23	31.8	0	10.46	19.19	0	27.04	45.06
AlF_3	63.56	50.44	27.82	65.05	50.67	20.47	73.12	61.55	41.95
Al	1.22	5.21	11.22	0.77	5.28	15	0	0	12.97
Graphite	4.82	2.16	1.32	3.96	1.8	1.2	26.87	11.40	0
$Al_xF(OH)_{3-x}$	2.76	0.25	0	1.98	0	0	-	-	-
Amorphous	26.48	31.87	27.83	28.25	31.79	34.14	-	-	-

3.6. Sensitivity testing

Impact and friction tests were done in order to determine the safety limits of the formulations. The results shown in Table 4 conform to the requirements set out in STANAG 4487 and EN 13631-4:2002 for impact sensitivity. Friction tests showed that all compositions were insensitive (> 360 N) to friction.

Table 4. Impact test results of compositions containing magnalium, flake-like aluminium particles and spherical aluminium particles.

	Magnalium	**Al flake**	**Al atomised**
Mass (kg)	5	10	10
H_{min} (cm)	54.8	94	88.2
E_{min} (J)	26.8	92.2	86.4

3.7. Mechanical Properties

The tensile elongation properties of pyrotechnic films filled with different particle morphologies are listed in Table 5. Tests using films filled with Al flake powder were only possible for filler loading up to 20 wt.%. It was not possible to prepare defect-free films at higher loadings. This limit was present at 50 wt.% loading for films filled with atomised aluminium powder. The presence of filler profoundly decreased the elongation to break. This decrease was more pronounced when using Al flake as filler particles.

Table 5. Tensile elongation-at-break (%) as a function of filler loading

	Wt. %	0	10	20	30	40	50
Fuel	Atomised	454	187	161	128	86	71
Type	Flake	454	140	69	-	-	-

4. Conclusions

Pyrotechnic time delay formulations based on the fluoropolymer Viton B filled with aluminium or magnalium powder can be prepared by a slurry casting process. Flexible films are obtained that are insensitive to ignition by friction or impact. Energy output can be as high as 8.3 MJ kg^{-1} and the open burn rate can reach 82 mm s^{-1}. Aluminium flakes as fuel burned faster than atomised aluminium but

they also had a more severe effect on mechanical property deterioration, i.e. decreasing the elongation at break.

Acknowledgements

This work is based on the research supported in part by AEL Mining Service and by the National Research Foundation of South Africa (Grant 83874). The opinions, findings and conclusions or recommendations expressed in this publication are those of the authors, and neither AEL Mining Services nor the NRF accept any liability whatsoever in this regard.

References

1. Mclain JH. Pyrotechnics from the viewpoint of solid state chemistry. Philadelphia: The Franklin Institute Press; 1980.
2. Conkling JAM, C. Chemistry of Pyrotechnics: Basic Principles and Theory. 2 ed. Boca Raton: CRC Press; 2011.
3. Bradley JN, Capey WD, Shere JF. Mechanism of reaction in metal+metal oxide systems [8]. Nature. 1979;277(5694):291-2. doi:10.1038/277291a0.
4. Charsley EL, Chen C-H, Boddington T, Laye PG, Pude JRG. Differential thermal analysis and temperature profile analysis of pyrotechnic delay systems: ternary mixtures of silicon, boron and potassium dichromate. Thermochimica Acta. 1980;35(2):141-52. doi:http://dx.doi.org/10.1016/0040-6031(80)87188-7.
5. Berger B. Parameters influencing the pyrotechnic reaction. Propellants, Explosives, Pyrotechnics. 2005;30(1):27-35. doi:10.1002/prep.200400082.
6. Booth F. The theory of self-propagating exothermic reactions in solid systems. Transactions of the Faraday Society. 1953;49(0):272-81. doi:10.1039/TF9534900272.
7. Margolis SB. A model for condensed combustion synthesis of nonstoichiometric homogeneous solids. Combustion and Flame. 1993;93(1-2):1-18. doi:10.1016/0010-2180(93)90080-M.
8. Margolis SB. Asymptotic theory of heterogeneous condensed combustion. Combustion science and technology. 1985;43(3-4):197-215.
9. Margolis SB. Asymptotic theory of condensed two-phase flame propagation. SIAM Journal on Applied Mathematics. 1983;43(2):351-69.
10. Margolis SB, Williams FA. Flame propagation in solids and high-density fluids with Arrhenius reactant diffusion. Combustion and Flame. 1991;83(3-4):390-8. doi:10.1016/0010-2180(91)90085-P.
11. Aldushin AP, Khaikin BI. Combustion of mixtures forming condensed reaction products. Combustion, Explosion, and Shock Waves. 1974;10(3):273-80. doi:10.1007/BF01463752.
12. Khaikin BI, Merzhanov AG. Theory of thermal propagation of a chemical reaction front. Combust Explos Shock Waves. 1966;2(3):22-7. doi:10.1007/BF00749022.
13. Puszynski J, Degreve J, Hlavacek V. Modeling of exothermic solid-solid noncatalytic reactions. Industrial and Engineering Chemistry Research. 1987;26(7):1424-34.